HHS Public Access

Author manuscript

Eur J Neurosci. Author manuscript; available in PMC 2015 October 01.

Published in final edited form as:

Eur J Neurosci. 2014 October ; 40(7): 3067–3077. doi:10.1111/ejn.12669.

Testing the role of preBötzinger complex somatostatin neurons in respiratory and vocal behaviors

Srinivasan Tupal[1], **Michael A. Rieger**[2,3], **Guang-Yi Ling**[1], **Thomas J. Park**[4], **Joseph D. Dougherty**[2,3], **Ann K. Goodchild**[5], and **Paul A. Gray**[1]

[1]Department of Anatomy and Neurobiology, Washington University School of Medicine, St. Louis, Missouri 63110, USA

[2]Department of Genetics, Washington University School of Medicine, St. Louis, Missouri 63110, USA

[3]Department of Psychiatry, Washington University School of Medicine, St. Louis, Missouri 63110, USA

[4]Laboratory of Integrative Neuroscience and Department of Biological Sciences, University of Illinois at Chicago, Chicago, IL, USA

[5]The Australian School of Advanced Medicine, Macquarie University Sydney, NSW, 2109, Australia

Abstract

Identifying neurons essential for the generation of breathing and related behaviors such as vocalization is an important question for human health. The targeted loss of preBötzinger complex (preBötC) glutamatergic neurons, including those that express high levels of somatostatin protein (SST neurons), eliminates normal breathing in adult rats. Whether preBötC SST neurons represent a functionally specialized population is unknown. We tested the effects on respiratory and vocal behaviors of eliminating SST neuron glutamate release by Cre-Lox-mediated genetic ablation of the vesicular glutamate transporter 2 (VGlut2). We found the targeted loss of VGlut2 in SST neurons had no effect on viability *in vivo*, or on respiratory period or responses to neurokinin 1 or μ-opioid receptor agonists *in vitro*. We then compared medullary SST peptide expression in mice with that of two species that share extreme respiratory environments but produce either high or low frequency vocalizations. In the Mexican free-tailed bat, SST peptide-expressing neurons extended beyond the preBötC to the caudal pole of the VII motor nucleus. In the naked mole-rat, however, SST-positive neurons were absent from the ventrolateral medulla. We then analyzed isolation vocalizations from SST-Cre;VGlut2$^{F/F}$ mice and found a significant prolongation of the pauses between syllables during vocalization but no change in vocalization number. These data suggest that glutamate release from preBötC SST neurons is not essential for breathing but play a species- and behavior-dependent role in modulating respiratory networks. They further suggest

Correspondence to Paul A. Gray, Department of Anatomy and Neurobiology, Washington University School of Medicine, Box 8108, 660 S. Euclid Ave, St. Louis, MO 63110, Fax: 314-362-3446, pgray@pcg.wustl.edu.

Conflict of Interest: The authors declare no conflicts of interest.

that the neural network generating respiration is capable of extensive plasticity given sufficient time.

Keywords

respiratory rhythm; vocalization; bat; naked mole-rat; preBötzinger complex

Introduction

The preBötzinger Complex (preBötC) has been identified as a region necessary and sufficient for the endogenous rhythmic respiratory-related output generated in isolated neonatal rodent hindbrain preparations (Smith *et al.*, 1991). Synaptic glutamate release from vesicular glutamate transporter 2 (VGlut2)-expressing neurons within the preBötC is necessary for the expression of respiratory behaviors both *in vivo* and *in vitro* (Greer *et al.*, 1991; Wallen-Mackenzie *et al.*, 2006; Wallen-Mackenzie *et al.*, 2010). In addition to glutamate, hindbrain neurons release other neurotransmitters including GABA and serotonin, and neuromodulators such as somatostatin (SST) and substance P (SP). However, the blockade or genetic elimination of these other neurotransmitters and neuropeptides does not eliminate respiratory rhythm (Low *et al.*, 2001; Telgkamp *et al.*, 2002; Hodges *et al.*, 2008).

Within mouse and rat preBötC, partially overlapping subsets of glutamatergic neurons can be genetically identified by their expression of SST, as well as the neurokinin 1 receptor (NK1R), SST 2a receptor (SST2aR) or μ-opioid receptor (μOR) (Gray *et al.*, 1999; Stornetta *et al.*, 2003; Llona *et al.*, 2004; Gray *et al.*, 2010). In adult rats, the near complete (≥ 80%) targeted ablation of preBötC NK1R neurons, many of which express SST, leads to ataxic breathing during wakefulness and cessation of breathing during sleep (Gray *et al.*, 2001; McKay & Feldman, 2008). The reversible genetic silencing of preBötC neurons transfected with an SST promoter-driven inhibitory G-protein-coupled receptor induces a rapid and prolonged apnea in otherwise normal awake animals (Tan *et al.*, 2008).

These data suggest an essential role for glutamatergic preBötC neurons in the generation of breathing (Feldman *et al.*, 2013). What is unclear, however, is whether the effects on breathing from the selective elimination or hyperpolarization of subsets of preBötC neurons are caused by the elimination of a specific subset of neurons essential for breathing or by a more general disruption of the connectivity of the respiratory network. We hypothesized that if preBötC SST neurons represent genetically specified essential components of the respiratory network, the elimination of their ability to release glutamate during late development should have profound effects on breathing and perhaps other brainstem-mediated behaviors such as vocalization (Jürgens, 2009).

We generated SST-Cre;VGlut2$^{F/F}$ mice to eliminate glutamatergic release from preBötC and other SST-expressing neurons to test the role of preBötC SST neurons in respiration. We then tested whether medullary cell-body SST expression was evolutionarily conserved in naked mole-rat and bat, two species that experience extremes of hypoxia and hypercapnia but vary in the spectral frequency of their vocalizations (Rubsamen, 1987; Credner *et al.*,

1997). We then compared isolation vocalizations in wild-type and SST-Cre;VGlut2$^{F/F}$ neonatal mice.

Together, these data are inconsistent with a genetically predetermined role for preBötC SST neurons for producing respiratory rhythm, as these neurons are neither essential for breathing nor evolutionarily conserved. The ability of the respiratory network to function with fewer glutamatergic neurons is consistent with recent work showing shared electrophysiological properties and developmental lineage amongst glutamatergic respiratory neurons of the ventrolateral medulla (VLM) as well as evolving models of respiratory rhythm generation (Feldman *et al.*, 2013).

Materials and methods

Animals

The study utilized *Dbx1*$^{LacZ/+}$, Rosa26; flox-stop-flox-Td Tomato (Rosa TD-Tomato), SST-Cre and VGlut2 flox-stop-flox (VGlut2$^{F/F}$) transgenic mice and controls, which were either littermates or age-matched CD1 mice (Pierani *et al.*, 2001; Madisen *et al.*, 2010; Rossi *et al.*, 2011; Taniguchi *et al.*, 2011). Mice were crossed and bred on a C57BL6 or mixed CD1/C57BL6 background. Naked mole-rats were 1 year old, raised in the laboratory. Maximum life span in naked mole-rats is approximately 30 years; the animals used here are considered to be young adults. Mexican free-tailed bats were caught in the wild as adults.

All the experiments were done in accordance with guidelines laid down by the NIH in the US regarding the care and use of animals for experimental procedures, the Institute for Laboratory Animal Research Guide for the Care and Use of Laboratory Animals, and in compliance with protocols approved by the Animal Studies Committee at Washington University School of Medicine and the University of Illinois at Chicago Institutional Animal Care and Use Committee.

Electrophysiology

Hindbrain–spinal cord (en bloc) preparations (Feldman & Smith, 1989) were dissected out by performing craniotomy and laminectomy on embryonic day (E)18.5 [SST-Cre;VGlut2$^{F/F}$, n=2 and control (CD1, n=3 and VGlut2$^{F/F}$, n=1)] and postnatal day 0 (P0) [SST-Cre;VGlut2$^{F/F}$, n=10, and control (CD1, n=4, VGlut2$^{F/+}$, n=3, VGlut2$^{F/F}$, n=1 and SST-Cre;VGlut2$^{F/+}$, n=1)] mouse pups while submerged under cold (4°C) artificial cerebral spinal fluid [aCSF; in mM: NaCl, 124; KCl, 3; $CaCl_2$, 1.5; $MgSO_4$, 1.0; $NaHCO_3$, 25.0; NaH_2PO_4, 0.5; and D-glucose, 30 (Sigma, St Louis, MO, USA) equilibrated with 95% O_2 and 5% CO_2 to pH = 7.4]. In P0 mouse pups the rostral transection was made at the pontomedullary junction and in the E18.5 pups it was done near the diencephalon–midbrain junction. Likewise, the caudal spinal transections in the P0 and E18.5 mouse pups were done in the thoracic and sacral regions, respectively. These preparations were then transferred into a 6-ml recording chamber which was gravity-fed by reservoirs of heated (25–26°C) and aerated (95% O_2 and 5% CO_2) aCSF at a rate of 6 ml/min. The preparations were allowed to stabilize for ~30 min and then extracellular electrophysiological recordings were made (acquisition rate 4 kHz) from cervical (C2–C6) ventral spinal motor roots using suction

electrodes. The signal was differentially amplified with a low-noise Grass Instruments (bandpass filtering, 0.3–3 kHz), digitized using an analog to digital converter (AD instruments, Colorado Springs, CO, USA) and integrated over time (absolute value with a 100-ms decay time-constant) using LabChart 7 Pro software (version 7.2.4, AD Instruments). After recording baseline activity for >30 minutes, 1 μM SP or 500 nM [D-Ala2, N-Me-Phe4, Gly5-ol]-enkephalin acetate salt (DAMGO) in aCSF was applied for 30 minutes into the recording chamber to study their effects on inspiratory rhythm. The peak time of each integrated respiratory burst (absolute value integral decay time constant, 100 ms) was determined and from this the inter-burst interval (period) was calculated. Each period was then normalized to the average baseline period for ease of comparison. These normalized periods, as well as irregularity scores (S_n= absolute value of $(P_n - P_{n-1})/P_{n-1}$, where S_n is the score of the nth cycle, P_n represents its period and P_{n-1} is the period of the preceding burst; Ramírez-Jarquín *et al.*, 2012), were then used to compare between the genotypes and for studying the effect of peptides on respiratory rhythm. All compounds were acquired from Sigma-Aldrich, St Louis, MO, USA unless otherwise noted.

Ultrasonic vocalization recording and analysis

VGlut2$^{F/F}$, SST Cre;VGlut2$^{F/+}$ and SST Cre;VGlut2$^{F/F}$ pups were separated from their dam on P8 and maintained between 32 and 34°C using a heating pad. Pups were individually recorded in a custom sound-attenuating chamber using an ultrasonic microphone (Avisoft Bioacoustics CM16) placed 20 cm above the pup, and a pre-amplifier/analog-to-digital converter (Avisoft Bioacoustics USGH116), and using USGH Recorder software (Avisoft Bioacoustics; digitized at 250kHz sampling, 16-bit signed integers, gain 1.4 dB) for 3 minutes, after which sex and weight were determined and tail tissue was removed for DNA extraction. Frequency domain data were determined from the digitized audio files in MATLAB (Mathworks, Natick, MA, USA; FFT window length, 512; 50% time overlap; frequency resolution, 488.3 Hz; time resolution, 1.024 ms), truncated to frequencies between 40 and 120 kHz. Ultrasonic syllable start and end times were automatically scored from the frequency domain data using software written by Timothy Holy (Holy & Guo, 2005). Using annotated syllable start and end times, custom scripts in MATLAB were used to calculate the total number of syllables uttered, syllable duration, mean syllable peak (fundamental) frequency and intersyllabic pause length. We set an arbitrary upper bound cutoff for within-phrase pauses of 240 ms by visual inspection of the pause times distribution of the combined data from all genotypes (4037 pauses; Figure 5B). To determine syllable power, the RMS voltage of the time domain data was determined for every syllable (512 sample window, 50% time overlap) and power was computed as V_{rms}^2 and time-averaged for each syllable. Power in Fig. 5 and in the text is expressed in dbV units where $dbV = 10 \times Log(V_{rms}^2/ref)$ where $ref = 1 \times V^2$. To normalize for differences in numbers of syllables between animals, duration, within-phrase pause, between-phrase pause and power were averaged over all such measurements for each animal, and hypothesis tests were conducts on these mean values.

Statistics

The normalized inspiratory periods and irregularity scores were compared using independent samples *t*-tests with the statistically significant difference set at $p< 0.05$. Differences in features of vocalization were determined by one-way ANOVA. Significant

differences ($p < 0.05$) between groups were followed with Bonferroni-corrected *post hoc* pairwise comparisons.

Immunohistochemistry

Tissue sections were washed in phosphate-buffered saline (PBS) with 0.2% triton X-100, blocked in 10% heat-inactivated normal horse sera, incubated in antibody overnight at 4°C, incubated in secondary antibody and coverslipped in Vectashield (Vector Laboratories, Burlingame, CA, USA).

Antibodies

Chicken anti-beta galactosidase (LacZ), 1:4000 (Abcam, Cambridge, MA, USA), rabbit anti-NK1R, 1:2000 (Millipore, Billerica, MA, USA), rabbit anti-Paired Box 2 (Pax2), 1:250 (Life Technologies, Grand Island, NY, USA), goat anti-RFP, 1:2000 (Rockland, Gilbertsville, PA, USA), goat anti-SST, 1:600 (Santa Cruz Biotechnology, Santa Cruz, CA, USA) and guinea pig anti-SST2aR, 1:10 000 (Gramsch Laboratories, Schwabhausen, Germany). Antibody specificity has either been shown previously or by comparison of antibody staining in transgenic mice lacking the target protein (Low *et al.*, 2001; Gray *et al.*, 2010).

In situ *hybridization*

Slides were immersed in 4% paraformaldehyde (PFA) in 0.1 M PBS, permeabilized with radioimmunoprecipitation assay buffer, washed in 0.1 M triethanolamine–HCl with 0.25% acetic anhydride, blocked in hybridization buffer at 65°C, then placed into slide mailers containing hybridization buffer with digoxigenin-labeled antisense VGlut2 cRNA at 1 μg/ml overnight at 65°C. Slides were washed in sodium citrate buffers at 62°C, then washed and incubated in alkaline phosphatase-conjugated anti-DIG antibody in 10% normal horse serum and incubated in nitro blue tetrazolium chloride and 5-bromo-4-chloro-3-indolyl phosphate (NBT-BCIP; Roche, Indianapolis, IN, USA) until cellular labeling was clear. For combined immunohistochemistry and *in situ* hybridization, slides were stained for mRNA expression prior to immunohistochemical labeling as previously described (Gray, 2013). All compounds were acquired from Sigma-Aldrich, St Louis MO, USA.

Genotyping

Mice were genotyped by PCR using primers specific for Cre recombinase, *Dbx1*^{LacZ}, TD-Tomato or VGlut2^{F} as previously described (Pierani *et al.*, 2001; Tong *et al.*, 2007; Madisen *et al.*, 2010; Taniguchi *et al.*, 2011).

Tissue acquisition

Neonatal pups (P0) or E18.5 embryos from timed pregnant females (morning of plug = E0.5) were anesthetized and perfused with 4% PFA in 0.1 M PBS, pH 7.4. Embryos or isolated hindbrains were postfixed in PFA overnight at 4°C, cryoprotected in 25% sucrose in PBS, blocked, frozen in OCT and stored at −75°C. Hindbrains were sectioned in sets of six on a Hacker (Winnsboro, SC, USA) cryostat at 20 μm and sections were thaw-mounted onto

Superfrost Plus (Fisher Scientific, Hampton, NH, USA) slides and stored at −20° C until use.

IHC and ISH image acquisition

Fluorescent and brightfield images were acquired using a Nikon 90i microscope (Nikon Instruments, Melville, NY, USA), Roper H_2-cooled CCD camera (Photometrics, Tucson, AZ, USA) and Optigrid structured illumination confocal with a Prior (Rockland, MA, USA) motorized translation stage. Pseudo-colored images were acquired in Velocity (Perkin Elmer, Waltham, MA, USA), and modified in Photoshop (Adobe, San Jose, CA, USA) or ImageJ (NIH, Bethesda, MD, USA) (Schneider *et al.*, 2012) and exported as 8-bit JPEG images. Images were filtered and levels were modified for clarity.

Results

Ontogeny of medulla SST expression

To determine whether SST expression was unique to the preBötC, we analyzed the localization of SST peptide within the medulla during development. By E12.5, after the bulk of medullary neurogenesis but prior to the onset of respiratory behaviors, SST was expressed in multiple populations along the dorsolateral edge of the medulla including within the developing spinal trigeminal nucleus (SpV) as well as by discrete subsets of interneurons within the developing reticular formation (Greer *et al.*, 1992; Greer *et al.*, 1999; Thoby-Brisson *et al.*, 2005; Gray, 2013). At this age, we found no expression of SST peptide in *Developing Brain Homeobox 1* (*Dbx1*)-derived, LacZ-expressing neurons within the preBötC but clear co-expression within probable inhibitory $LacZ^{-}Pax2^{+}$ neurons (Fig. 1A; also Gray, 2013). By E15.5, however, SST expression was limited to the preBötC, the nucleus of Roller and within the SpV (Figure 1B). This matches the localization of preproSST mRNA (Figure 1C). As a consequence of the transient expression of SST during development, we found broad TD-Tomato expression in E15.5 SST-Cre;Rosa TD-Tomato transgenic mouse medulla including within preBötC SST neurons (Figs 1B and 2B and C). By P0, SST peptide-immunopositive terminals were broadly located throughout the medulla. SST neurons, however, continued to be limited to the nucleus of Roller (not shown) and to a subpopulation of *Dbx1*-derived neurons within the preBötC (Figure 2A and C).

SST-Cre-mediated elimination of glutamate release in preBötC SST neurons

We tested whether SST-Cre could eliminate VGlut2 expression within preBötC SST neurons in SST-Cre;$VGlut2^{F/F}$ mice. In perinatal control mice, 77% of preBötC SST^{+} neurons showed clearly detectable levels of VGlut2 mRNA (17/22 neurons, n=2 animals; Figure 2D) consistent with results from rats and the glutamatergic phenotype of preBötC *Dbx1*-derived neurons (Stornetta *et al.*, 2003; Bouvier *et al.*, 2010; Gray *et al.*, 2010). In P0 SST-Cre;$VGlut2^{F/F}$ mice, in contrast, only 3.5% of preBötC SST^{+} neurons expressed VGlut2 mRNA (3/85 neurons, n=4 animals; Figure 2E). We found no obvious change in the SST neuron number or in VGlut2 co-expression with Pax2 in non-SST neurons between P0 wild-type and SST-Cre;$VGlut2^{F/F}$ mice (Fig. 2D and E). Thus, by birth nearly all preBötC SST^{+} neurons in SST-Cre;$VGlut2^{F/F}$ mice lacked detectable vesicular glutamate transporter

mRNA expression, a gene essential for synaptic glutamate release, but still showed robust SST protein staining.

Effect of the elimination of glutamate release in preBötC SST$^+$ neurons on breathing in vitro

To test the necessity of glutamate release from preBötC SST neurons for breathing, we utilized SST-Cre;VGlut2$^{F/F}$ crosses. Both at E18.5 and at birth, these animals were viable and behaviorally indistinguishable from their control littermates. They were capable of growing to adulthood and reproducing. We isolated the medulla and spinal cord from E18.5 (not shown) and P0 SST-Cre;VGlut2$^{F/F}$ and control mice to a recording chamber and recorded endogenous inspiratory output from C3–4 motor roots. Both control and SST-Cre;VGlut2$^{F/F}$ mice generated endogenous inspiratory-like rhythms from cervical roots (Fig. 3A, C, E and G). We found no difference in baseline period [control mice, 1.0000 ± 0.07643 (SEM, n=4); SST-Cre;VGlut2$^{F/F}$, 1.0116 ± 0.05291, n=5; $p<0.902$]. We also found no difference in the regularity of respiratory output (irregularity scores: control mice, 1.0000 ± 0.14191, n=4; SST-Cre;VGlut2$^{F/F}$, 1.0951± 0.10465, n=5; $p<0.595$) (Ramírez-Jarquín *et al.*, 2012). These results indicate glutamatergic transmission from preBötC SST neurons is not essential for respiratory rhythmogenesis or stability *in vitro*.

We tested the effects of bath application of either the μOR agonist DAMGO (1μM) or SP (1 μM). DAMGO caused the cessation of inspiratory rhythm within 5 min in both control (4.4 ± 2.4 minutes; Figure 3B) and SST-Cre;VGlut2$^{F/F}$ (4.3 ± 1.4 minutes; Figure 3F) animals. In contrast, SP significantly decreased respiratory periods from baseline in both animals (control mice, 0.8829 ± 0.03885, n=4, $p<0.032$; SST-Cre;VGlut2$^{F/F}$, 0.846± 0.0276, n=5, $p<4.6 \times 10^{-4}$; Fig. 3D and H). These data suggest preBötC SST neurons are not the sole mediators of peptidergic modulation of respiratory frequency within the hindbrain, at least at the dosages used (Montandon *et al.*, 2011; Lalley *et al.*, 2014; Montandon & Horner, 2014).

Comparative analysis of preBötC SST expression

Within the cortex, SST expression identifies an evolutionarily conserved population of inhibitory interneurons (Wonders & Anderson, 2006; Tanaka *et al.*, 2011). Because the loss of synaptic glutamate release from preBötC SST neurons had no significant effects on *in vitro* respiratory output, we wondered whether preBötC SST expression was evolutionarily conserved or correlated with environment or behavior. Both bats and naked mole-rats live, for periods, in underground chambers and experience high levels of CO_2, low levels of oxygen and high levels of ammonia (Brett, 1991; Elliott, 1993; Bennett & Faulkes, 2000). Their extensive vocal productions in their nesting environments, however, are very different, with the mole-rat exhibiting low frequency vocalizations and hearing in contrast to the high frequency vocalizations used in mouse and most notably in bats (Pepper *et al.*, 1991; Heffner & Heffner, 1993; Yosida *et al.*, 2007; Bohn *et al.*, 2008).

The preBötC lies within the evolutionarily conserved VLM, ventral to the nucleus ambiguus (NA) between the rostral pole of the lateral reticular nucleus and the caudal pole of the compact NA (Smith *et al.*, 1991; Gray *et al.*, 1999; Cambronero & Puelles, 2000; Marin *et al.*, 2008; Gray, 2013). To determine whether SST expression was conserved in different

mammals we performed immunohistochemistry against SST within the medulla of adult Mexican free-tailed bats (n=5) and naked mole-rats (n=3). In bats, SST positive fibers were densely located within the nucleus tractus solitarius (NTS) and were scattered within the VLM and the intermediate reticular formation (Figure 4A). SST-positive neurons within the VLM, however, extended from the caudal pole of the NA to the caudal pole of the facial motonucleus (VII; Fig. 4B and C), which in mouse encompasses multiple distinct respiratory regions including the rostral ventral respiratory group (VRG), the preBötC and the parafacial respiratory group (pFRG) (Onimaru & Homma, 2003; Alheid & McCrimmon, 2008; Feldman *et al.*, 2013). In mice, the majority of preBötC SST neurons co-expressed SST2aR, consistent with an inhibitory role of SST on respiratory output (Burke *et al.*, 2010; Gray *et al.*, 2010). In the bat, similar co-expression was seen along the full rostrocaudal extent of SST expression (Figure 5, n=4). Also similar to mice and rat, SST2aR is expressed by non-SST-expressing neurons within the ventrolateral medulla (Burke *et al.*, 2008; Gray, 2013).

In naked mole-rats, dense SST fiber expression was found within the dorsal motor nucleus of the vagus and within the NTS (Figure 4D). We also found diffuse SST terminals within the VLM. We did find strongly SST-immunoreactive neurons within the raphe obscurus 5-hydroxytryptamine (5-HT)-expressing population, unlike in rats, cats or mice but consistent with guinea pig (Fig. 4D–F) (Johansson *et al.*, 1984; Taber-Pierce *et al.*, 1985; De Leon *et al.*, 1992; Stornetta *et al.*, 2003; Llona & Eugenin, 2005). The few SST^+ neurons present in the VLM co-expressed 5-HT (Figure 4E). Similar to mice and rats, we found no medullary co-expression of SST with tyrosine hydroxylase in bats or naked mole-rats (Figures 4B and E) (Stornetta *et al.*, 2003; Llona & Eugenin, 2005; Bouvier *et al.*, 2010; Gray *et al.*, 2010). Together these data suggest that preBötC SST expression is not conserved within mammalian species, even within the order Rodentia. They further suggest that, within the hindbrain, SST expression is strongly species-specific.

Role of preBötC SST neurons in ultrasonic vocalization

It has been proposed that SST expression plays a role in protecting the respiratory network from excessive activation, such as during hypoxia or hypercapnia (Llona *et al.*, 2004; Ramírez-Jarquín *et al.*, 2012). Given the presence of SST neurons within the medulla of animals that produce high frequency vocalizations, we hypothesized that vocalization may also stress the respiratory network and that the elimination of glutamatergic release from preBötC SST neurons may modulate vocalization to a greater extent than the baseline respiratory rhythm. In rats and also probably in mice, ultrasonic (>40 kHz) calls, often described as ‘whistles’, are accompanied by strong activation of laryngeal muscles innervated by motoneurons of the NA (Bieger & Hopkins, 1987; Riede, 2013). Although the primary source(s) of the drive to these motoneurons during vocalization are currently unknown, first order premotor neurons and vocalization active neurons are located within respiratory regions of the medulla (Holstege, 1989; Chiao *et al.*, 1994; Larson *et al.*, 1994; Jurgens & Hage, 2007; Van Daele & Cassell, 2009; Van Daele *et al.*, 2011).

In response to separation from their dam, mouse pups vocalize ultrasonically in bouts of activity separated by periods of silence as shown in Fig 6A (Hofer *et al.*, 2002; Gourbal *et*

al., 2004; Portfors, 2007.) These bouts of behavior are composed of individual calls that have an average duration of ~50 ms (Fig. 6A, right) and have been hypothesized to represent phrases of song composed of individual syllables, using terminology from birdsong (Holy & Guo, 2005). Syllables are composed of primarily narrow frequency bands, distinguishing them from other types of sounds, which are broadband (not shown). Figure 6A shows a sound spectrogram ('sonogram') of isolation vocalizations from a P8 mouse. We compared numbers of whistles between VGlut2$^{F/F}$ (n=18), SST-Cre;VGlut2$^{F/+}$ (n = 7) and SST-Cre;VGlut2$^{F/F}$mice (n=13). We found no significant differences between genotypes in the number of syllables per recording session (VGlut2$^{F/F}$, 101±17; SST-Cre;VGlut2$^{F/+}$, 91±23; SST-Cre;VGlut2$^{F/F}$, 116±26; means ± SEM, one-way ANOVA, $F_{2,36} = 0.26$, $p = 0.77$), indicating that groups did not exhibit significant differences in overall behavioral response to maternal isolation.

Given the hypothesized role of preBötC neurons in the production of respiratory behaviors, we examined both temporal and spectral features of whistles. Mean whistle duration did not differ significantly between groups (VGlut2$^{F/F}$, 64.6 ± 0.9 ms; SST-Cre;VGlut2$^{F/+}$, 65.0±1.6 ms; SST-Cre;VGlut2$^{F/F}$, 64.8 ± 1.0 ms; one-way ANOVA, $F_{2,36} = 0.03$, $p = 0.97$). We also found no significant differences between the mean fundamental frequencies of syllables (VGlut2$^{F/F}$, 68.1 ± 1.4 kHz; SST-Cre;VGlut2$^{F/+}$, 71.4±2.6 kHz; SST-Cre;VGlut2$^{F/F}$, 72.0 ± 1.2 kHz; one-way ANOVA, $F_{2,36} = 2.01$, $p = 0.15$). We also compared whether the average power of each whistle, which is proportional to loudness, was different between groups. We calculated the power over each whistle (Fig. 6E and F) and found no significant differences between groups, indicating that the loss of glutamate release from preBötC SST neurons does not affect the vocalization intensity (VGlut2$^{F/F}$, –48.5 ± 1.5 dBV; SST-Cre;VGlut2$^{F/+}$, –52.5 ± 1.6 dBV; SST-Cre;VGlut2$^{F/F}$, –49.0 ± 1.9 dBV; one-way ANOVA, $F_{2,36} = 1.17$, $p = 0.32$).

We then examined pause times between whistles. Pauses between whistles occur as highly variable long pauses between phrases of vocalization which span several orders of magnitude and short pauses between syllables of a phrase which are more tightly distributed (Fig. 6B). In particular, intersyllabic pauses occurring within a phrase may represent the murine correlate to so-called mini-breaths, or short inspirations, observed in vocalization of rats and birds (Wild *et al.*, 1998; Riede, 2013). We found that mean intersyllabic pause within phrase in both SST-Cre;VGlut2$^{F/F}$ and SST-Cre;VGlut2$^{F/+}$ animals was significantly increased (Fig. 6C; VGlut2$^{F/F}$, 30.1 ± 2.1 ms; SST-Cre;VGlut2$^{F/+}$, 146.4 ± 7.4 ms; SST-Cre;VGlut2$^{F/F}$, 141.3 ± 4.1 s; one-way ANOVA, $F_{2,35} = 4.80$, $p = 0.014$. One control animal was excluded as it only exhibited 12 phrases, each composed of a single syllable.). Bonferroni-corrected *post hoc* comparisons revealed a significant difference between control animals and both SST-Cre;VGlut2$^{F/+}$ ($p = 0.01$) and SST-Cre;VGlut2$^{F/F}$ ($p = 0.02$). We did not find a significant change to average length of pauses between phrases (Vglut2$^{F/F}$, 4.8 ± 1.3 s; SST-Cre;VGlut2$^{F/F}$, 4.1 ± 1.0 s; SST-Cre;VGlut2$^{F/F}$, 4.0 ± 0.7 s; Fig. 6D). Taken together, the lengthening of pause times is consistent with effects on the networks controlling inspiratory output and an absence of effects on motivational networks initiating vocalizations.

Discussion

Identifying exactly which neurons generate the mammalian breathing rhythm is an important question for both neuroscience and human health (Feldman *et al.*, 2013). The last 20 years have seen the identification of neurons essential for the expression of respiratory behaviors become progressively more specific. The preBötC was found to be necessary and sufficient for the inspiratory rhythm generation in perinatal rodent *in vitro* preparations (Smith *et al.*, 1991). This region contains partially overlapping populations of SST-, NK1R-, SST2aR- and/or μOR-expressing glutamatergic neurons (Gray *et al.*, 1999; Stornetta *et al.*, 2003; Gray *et al.*, 2010). SST affects breathing both *in vivo* and *in vitro* in mammals as well as amphibians, and plays an important role in stabilizing breathing in response to hypoxia (Llona *et al.*, 2004; Kinkead, 2009; Burke *et al.*, 2010; Ramírez-Jarquín *et al.*, 2012). SST signaling within the preBötC is not essential for breathing as mice with a targeted deletion of SST peptide or SST2a receptors are viable and breed (Low *et al.*, 2001; Allen *et al.*, 2003). The anatomical specificity of preBötC SST neurons and the functional consequences on breathing of the absence of SST signaling within the preBötC suggest a relationship between these neurons and breathing (Low *et al.*, 2001; Ramírez-Jarquín *et al.*, 2012).

PreBötC SST neurons in perinatal and adult mice express multiple neuropeptide receptors including NK1R, SST2aR and probably μOR, although they are not exclusive to those neurons (Burke *et al.*, 2010; Gray *et al.*, 2010; Gray, 2013). The targeted ablation, over several days, of preBötC NK1R-expressing neurons in adult rats leads to ataxic breathing during wakefulness and apnea during sleep (Gray *et al.*, 2001; McKay & Feldman, 2008). The acute hyperpolarization of preBötC neurons transfected with an invertebrate inhibitory G-protein-coupled receptor driven by a fragment of the SST promoter leads to complete apnea (Tan *et al.*, 2008). Together these experiments suggest an important, if not essential, role for preBötC SST-expressing glutamatergic neurons (Feldman *et al.*, 2013).

There are several possible interpretations for these *in vivo* results. One is that that a genetically specified population of preBötC SST neurons generates or is somehow otherwise essential for the respiratory rhythm. Our results show this is clearly incorrect, as the elimination of glutamate release in these neurons by Cre-mediated ablation of vesicular glutamate packaging, prior to birth, has no effect on viability *in vivo* or on respiratory period or neuropeptide modulation *in vitro*. Alternately, the preBötC SST population may only represent a subset of a larger essential population, e.g. NK1R-expressing neurons. Consistent with this, viral transfection of preBötC neurons using an SST promoter labeled a larger population than expected based on the number of SST neurons within the preBötC (Stornetta *et al.*, 2003; Tan *et al.*, 2008). As the SST-Cre transgene clearly also labels many preBötC neurons that lack detectable SST protein, we consider this simple numerical interpretation unlikely.

We suggest that the acute ablation or hyperpolarization of a subpopulation of preBötC neurons may affect the ability of the remaining respiratory network to propagate sufficient excitability to produce a consistent respiratory output leading to apnea and death (Del Negro *et al.*, 2002; Gray *et al.*, 2010; Hayes *et al.*, 2012; Feldman *et al.*, 2013). In this case, disrupting breathing simply requires the sudden loss of a sufficient population with a given

connectivity, perhaps within a specific region. This hypothesis is supported by evidence from studies done using brain slices in which the acute sequential ablation of randomly chosen preBötC neurons eventually leads to respiratory failure, as would be expected from a distributed respiratory network (Hayes *et al.*, 2012; Wang *et al.*, 2013) but the slow targeted ablation of preBötC NK1R neurons over the course of weeks in goats does not eliminate normal breathing (Wenninger *et al.*, 2004a; Wenninger *et al.*, 2004b; Krause *et al.*, 2009; Forster *et al.*, 2010). Our results suggest the respiratory network has sufficient plasticity to recover function given adequate time. Importantly, these results do not imply that in normal animals preBötC SST neurons play no role in respiratory rhythm generation, only that they do not represent a genetically defined essential population.

In contrast to the absence of effects on basal respiratory output, we found an unexpected modulation in the length of likely inspiratory pauses between syllables during vocalization, after maternal separation in SST-Cre;VGlut2$^{F/F}$ mice compared with control. It is hypothesized that rodent vocalization, similar to human and bird vocalization, is generated by circuits within the cortex because of the direct cortical innervation of vocal motoneurons (Jürgens, 2009; Arriaga *et al.*, 2012). In both rats and zebra finches, the pauses between syllables, also called mini-breaths, correspond to short inspirations. In the zebra finch, cooling of the cortex preferentially lengthens syllables as compared to mini-breaths, consistent with a role for the hindbrain in the timing of inspiratory pauses (Andalman *et al.*, 2011). We found a significant increase in the time between syllables corresponding to longer inspirations. Whether this is due to the loss of glutamate signaling from SST neurons or the maintenance of SST release in the absence of glutamate release is as yet unknown. These results are also consistent with distinct roles for the forebrain and hindbrain in vocalizations and suggest the analysis of vocalizations can differentiate between motor and motivational deficits (Dougherty *et al.*, 2013).

VGlut2 and SST are also co-expressed in the periventricular hypothalamus (PVH), hindbrain auditory pathways and peripheral ganglia of adult mice (Tachibana *et al.*, 1979; Helke & Hill, 1988; Hurley *et al.*, 1997; Smotherman, 2007). PVH neurons do project to the hindbrain; however, PVH SST expression does not begin until P3 and does not reach adult levels until after weaning. Similarly, P9 mice cannot hear high frequency sounds. Thus in both cases, glutamate release from central SST neurons outside the preBötC is unlikely to play an important role in vocalization at this age. SST is also expressed in VGlut2-expressing peripheral ganglia in adults so some aspects of mini-breath prolongation may be a consequence of changes in synaptic inputs from peripheral stretch or chemoreceptors. Overall, we propose the prolongation of the inspiratory period is probably mediated by changes in glutamate release by SST neurons within the preBötC, consistent with their hypothesized role in inspiratory output.

What controls the expression of SST or other markers within the preBötC is unknown. We found that SST expression within the preBötC was not evolutionarily conserved in naked mole-rats and extended beyond its classic boundaries in bat. The co-expression of SST with SST2aR was conserved in bats, however. Recent work has suggested regions within the ventral respiratory column adjacent to the preBötC play important roles in the generation of more complex respiratory behaviors including sighing and expiration (Lieske *et al.*, 2000;

Mellen *et al.*, 2003; Lieske & Ramirez, 2006; Ruangkittisakul *et al.*, 2008; Doi & Ramirez, 2010; Mellen & Mishra, 2010; Mellen & Thoby-Brisson, 2012; Carroll *et al.*, 2013). The finding that within the bat medulla the most effective 'marker' for the preBötC extends the length of the VLM, combined with the finding that the majority of VLM glutamatergic respiratory neurons, including outside the preBötC, are derived from a single developmental progenitor domain, suggests that normal breathing and other breathing-related behaviors require the coordination of many neurons both within and outside the preBötC (Gray *et al.*, 2010; Gray, 2013; Tupal *et al.*, 2014).

Acknowledgments

This work was supported by National Heart, Lung, and Blood Institute Grant to S.T., G.L. and P.A.G. (R01HL089742), by NINDS (4R00NS067239-03) to J.D.D., National Health and Medical Research Council of Australia (APP1028183) to A.K.G. and P.A.G., and the National Science Foundation to T.J.P. (0744979). M.A.R. was supported by Kirschtein-NRSA (5T32GM007067-38). We thank Bradford Lowell for sharing the VGlut2$^{F/F}$ mice.

Abbreviations

μOR	μ-opioid receptor
5-HT	5-hydroxytryptamine
aCSF	artificial cerebral spinal fluid
DAMGO	[D-Ala2, N-Me-Phe4, Gly5-ol]-enkephalin acetate salt
Dbx1	Developing Brain Homeobox 1
E	embryonic day
LacZ	beta galactosidase
NA	nucleus ambiguus
NK1R	neurokinin 1 receptor
NTS	nucleus tracus solitarius
P	postnatal day
Pax2	Paired Box 2
PBS	phosphate-buffered saline
pFRG	parafacial respiratory group
preBötC	preBötzinger Complex
SP	substance P
SpV	spinal trigeminal nucleus
SST	somatostatin
SST2aR	SST 2a receptor
VGlut2	vesicular glutamate transporter 2

VGlut2$^{F/F}$	VGlut2 flox-stop-flox
VLM	ventrolateral medulla
VRG	ventral respiratory group

References

Alheid GF, McCrimmon DR. The chemical neuroanatomy of breathing. Respir Physiol Neurobiol. 2008; 164:3–11. [PubMed: 18706532]

Allen JP, Hathway GJ, Clarke NJ, Jowett MI, Topps S, Kendrick KM, Humphrey P, Wilkinson LS, Emson PC. Somatostatin receptor 2 knockout/lacZ knockin mice show impaired motor coordination and reveal sites of somatostatin action within the striatum. European Journal of Neuroscience. 2003; 17:1881–1895. [PubMed: 12752788]

Andalman AS, Foerster JN, Fee MS. Control of vocal and respiratory patterns in birdsong: dissection of forebrain and brainstem mechanisms using temperature. PLoS One. 2011; 6:e25461. [PubMed: 21980466]

Arriaga G, Zhou EP, Jarvis ED. Of mice, birds, and men: the mouse ultrasonic song system has some features similar to humans and song-learning birds. PLoS One. 2012; 7:e46610. [PubMed: 23071596]

Bennett, NC.; Faulkes, CG. African mole-rats: ecology and eusociality. Cambridge University Press; 2000.

Bieger D, Hopkins DA. Viscerotopic representation of the upper alimentary tract in the medulla oblongata in the rat: the nucleus ambiguus. Journal of Comparative Neurology. 1987; 262:546–562. [PubMed: 3667964]

Bohn KM, Schmidt-French B, Ma ST, Pollak GD. Syllable acoustics, temporal patterns, and call composition vary with behavioral context in Mexican free-tailed bats. The Journal of the Acoustical Society of America. 2008; 124:1838–1848. [PubMed: 19045674]

Bouvier J, Thoby-Brisson M, Renier N, Dubreuil V, Ericson J, Champagnat J, Pierani A, Chedotal A, Fortin G. Hindbrain interneurons and axon guidance signaling critical for breathing. Nature Neuroscience. 2010; 13:1066–1074.

Brett RA. The ecology of naked mole-rat colonies: burrowing, food, and limiting factors. The biology of the naked mole-rat. 1991:137–184.

Burke PG, Abbott SB, McMullan S, Goodchild AK, Pilowsky PM. Somatostatin selectively ablates post-inspiratory activity after injection into the Botzinger complex. Neuroscience. 2010; 167:528–539. [PubMed: 20149846]

Burke PG, Li Q, Costin ML, McMullan S, Pilowsky PM, Goodchild AK. Somatostatin 2A receptor-expressing presympathetic neurons in the rostral ventrolateral medulla maintain blood pressure. Hypertension. 2008; 52:1127–1133. [PubMed: 19001189]

Cambronero F, Puelles L. Rostrocaudal nuclear relationships in the avian medulla oblongata: a fate map with quail chick chimeras. The Journal of Comparative Neurology. 2000; 427:522–545. [PubMed: 11056462]

Carroll MS, Viemari J-C, Ramirez J-M. Patterns of inspiratory phase-dependent activity in the in vitro respiratory network. Journal of neurophysiology. 2013; 109:285–295. [PubMed: 23076109]

Chiao GZ, Larson CR, Yajima Y, Ko P, Kahrilas PJ. Neuronal activity in nucleus ambiguous during deglutition and vocalization in conscious monkeys. Experimental brain research. Experimentelle Hirnforschung. Experimentation cerebrale. 1994; 100:29–38.

Credner S, Burda H, Ludescher F. Acoustic communication underground: vocalization characteristics in subterranean social mole-rats (Cryptomys sp., Bathyergidae). Journal of Comparative Physiology A. 1997; 180:245–255.

De Leon M, Covenas R, Narrvaez J, Tramu G, Aguirre J, Gonzalez-Baron S. Distribution of somatostatin-28 (1,Äì12) in the cat brainstem: an immunocytochemical study. Neuropeptides. 1992; 21:1–11. [PubMed: 1346714]

Del Negro CA, Morgado-Valle C, Feldman JL. Respiratory rhythm: an emergent network property? Neuron. 2002; 34:821–830. [PubMed: 12062027]

Doi A, Ramirez JM. State-dependent interactions between excitatory neuromodulators in the neuronal control of breathing. J Neurosci. 2010; 30:8251–8262. [PubMed: 20554877]

Dougherty JD, Maloney SE, Wozniak DF, Rieger MA, Sonnenblick L, Coppola G, Mahieu NG, Zhang J, Cai J, Patti GJ. The disruption of Celf6, a gene identified by translational profiling of serotonergic neurons, results in autism-related behaviors. The Journal of Neuroscience. 2013; 33:2732–2753. [PubMed: 23407934]

Elliott, WR. Air monitoring during construction of a cave gate; Proceedings of the 1993 National Cave Management Symposium; Carlsbad, New Mexico. City. p. 45-51.Year

Feldman, JL.; Del Negro, C.; Gray, PA. Understanding the Rhythm of Breathing: So Near, Yet So Far. In: Julius, D.; Clapham, DE., editors. Annual Review of Physiology. Vol. 75. Palo Alto: 2013. p. 423-452.Annual Reviews

Feldman JL, Smith JC. Cellular mechanisms underlying modulation of breathing pattern in mammals. Annals of the New York Academy of Sciences. 1989; 563:114–130. [PubMed: 2476055]

Forster HV, Krause KL, Kiner T, Neumueller SE, Bonis JM, Qian B, Pan LG. Plasticity of respiratory rhythm-generating mechanisms in adult goats. Adv Exp Med Biol. 2010; 669:151–155. [PubMed: 20217339]

Gourbal BE, Barthelemy M, Petit G, Gabrion C. Spectrographic analysis of the ultrasonic vocalisations of adult male and female BALB/c mice. Naturwissenschaften. 2004; 91:381–385. [PubMed: 15278217]

Gray PA. Transcription Factors Define the Neuroanatomical Organization of the Medullary Reticular Formation. Frontiers in Neuroanatomy. 2013; 7

Gray PA, Hayes JA, Ling GY, Llona I, Tupal S, Picardo MC, Ross SE, Hirata T, Corbin JG, Eugenin J, Del Negro CA. Developmental origin of preBotzinger complex respiratory neurons. The Journal of Neuroscience : the official journal of the Society for Neuroscience. 2010; 30:14883–14895. [PubMed: 21048147]

Gray PA, Janczewski WA, Mellen N, McCrimmon DR, Feldman JL. Normal breathing requires preBotzinger complex neurokinin-1 receptor-expressing neurons. Nat Neurosci. 2001; 4:927–930. [PubMed: 11528424]

Gray PA, Rekling JC, Bocchiaro CM, Feldman JL. Modulation of respiratory frequency by peptidergic input to rhythmogenic neurons in the preBotzinger complex. Science. 1999; 286:1566–1568. [PubMed: 10567264]

Greer JJ, Allan DW, Martin-Caraballo M, Lemke RP. An overview of phrenic nerve and diaphragm muscle development in the perinatal rat. Journal of Applied Physiology. 1999; 86:779–786. [PubMed: 10066685]

Greer JJ, Smith JC, Feldman JL. Role of excitatory amino acids in the generation and transmission of respiratory drive in neonatal rat. J Physiol. 1991; 437:727–749. [PubMed: 1653855]

Greer JJ, Smith JC, Feldman JL. Respiratory and locomotor patterns generated in the fetal rat brain stem-spinal cord in vitro. J Neurophysiol. 1992; 67:996–999. [PubMed: 1588395]

Hayes JA, Wang X, Del Negro CA. Cumulative lesioning of respiratory interneurons disrupts and precludes motor rhythms in vitro. Proceedings of the National Academy of Sciences of the United States of America. 2012; 109:8286–8291. [PubMed: 22566628]

Heffner RS, Heffner HE. Degenerate hearing and sound localization in naked mole rats (Heterocephalus glaber), with an overview of central auditory structures. Journal of Comparative Neurology. 1993; 331:418–433. [PubMed: 8514919]

Helke C, Hill K. Immunohistochemical study of neuropeptides in vagal and glossopharyngeal afferent neurons in the rat. Neuroscience. 1988; 26:539–551. [PubMed: 2459628]

Hodges MR, Tattersall GJ, Harris MB, McEvoy SD, Richerson DN, Deneris ES, Johnson RL, Chen ZF, Richerson GB. Defects in breathing and thermoregulation in mice with near-complete absence of central serotonin neurons. J Neurosci. 2008; 28:2495–2505. [PubMed: 18322094]

Hofer MA, Shair HN, Brunelli SA. Ultrasonic vocalizations in rat and mouse pups. Current protocols in neuroscience. 2002:8.14. 11–18.14. 16. [PubMed: 18428573]

Holstege G. Anatomical study of the final common pathway for vocalization in the cat. Journal of Comparative Neurology. 1989; 284:242–252. [PubMed: 2754035]

Holy TE, Guo Z. Ultrasonic songs of male mice. PLoS biology. 2005; 3:e386. [PubMed: 16248680]

Hurley D, Wee B, Phelps C. Hypophysiotropic somatostatin expression during postnatal development in growth hormone-deficient Ames dwarf mice: mRNA in situ hybridization. Neuroendocrinology. 1997; 65:98–106. [PubMed: 9067987]

Johansson O, Hokfelt T, Elde RP. Immunohistochemical distribution of somatostatin-like immunoreactivity in the central nervous system of the adult rat. Neuroscience. 1984; 13:265–IN262. [PubMed: 6514182]

Jürgens U. The neural control of vocalization in mammals: a review. Journal of Voice. 2009; 23:1–10. [PubMed: 18207362]

Jurgens U, Hage SR. On the role of the reticular formation in vocal pattern generation. Behavioural brain research. 2007; 182:308–314. [PubMed: 17173983]

Kinkead R. Phylogenetic trends in respiratory rhythmogenesis: insights from ectothermic vertebrates. Respir Physiol Neurobiol. 2009; 168:39–48. [PubMed: 19505591]

Krause KL, Forster HV, Kiner T, Davis SE, Bonis JM, Qian B, Pan LG. Normal breathing pattern and arterial blood gases in awake and sleeping goats after near total destruction of the presumed pre-Botzinger complex and the surrounding region. J Appl Physiol. 2009; 106:605–619. [PubMed: 19095752]

Lalley PM, Pilowsky PM, Forster HV, Zuperku EJ. CrossTalk opposing view: The pre-Bötzinger complex is not essential for respiratory depression following systemic administration of opioid analgesics. The Journal of physiology. 2014; 592:1163–1166. [PubMed: 24634012]

Larson CR, Yajima Y, Ko P. Modification in activity of medullary respiratory-related neurons for vocalization and swallowing. Journal of neurophysiology. 1994; 71:2294–2304. [PubMed: 7931518]

Lieske SP, Ramirez JM. Pattern-specific synaptic mechanisms in a multifunctional network. I. Effects of alterations in synapse strength. J Neurophysiol. 2006; 95:1323–1333. [PubMed: 16492944]

Lieske SP, Thoby-Brisson M, Telgkamp P, Ramirez JM. Reconfiguration of the neural network controlling multiple breathing patterns: eupnea, sighs and gasps [see comment]. Nat Neurosci. 2000; 3:600–607. [PubMed: 10816317]

Llona I, Ampuero E, Eugenin JL. Somatostatin inhibition of fictive respiration is modulated by pH. Brain Research. 2004; 1026:136–142. [PubMed: 15476705]

Llona I, Eugenin J. Central actions of somatostatin in the generation and control of breathing. Biological Research. 2005; 38:347–352. [PubMed: 16579516]

Low MJ, Otero-Corchon V, Parlow AF, Ramirez JL, Kumar U, Patel YC, Rubinstein M. Somatostatin is required for masculinization of growth hormone,Äìregulated hepatic gene expression but not of somatic growth. Journal of Clinical Investigation. 2001; 107:1571–1580. [PubMed: 11413165]

Madisen L, Zwingman TA, Sunkin SM, Oh SW, Zariwala HA, Gu H, Ng LL, Palmiter RD, Hawrylycz MJ, Jones AR, Lein ES, Zeng H. A robust and high-throughput Cre reporting and characterization system for the whole mouse brain. Nat Neurosci. 2010; 13:133–140. [PubMed: 20023653]

Marin F, Aroca P, Puelles L. Hox gene colinear expression in the avian medulla oblongata is correlated with pseudorhombomeric domains. Developmental Biology. 2008; 323:230–247. [PubMed: 18786526]

McKay LC, Feldman JL. Unilateral ablation of pre-Botzinger complex disrupts breathing during sleep but not wakefulness. Am J Respir Crit Care Med. 2008; 178:89–95. [PubMed: 18420958]

Mellen NM, Janczewski WA, Bocchiaro CM, Feldman JL. Opioid-induced quantal slowing reveals dual networks for respiratory rhythm generation. Neuron. 2003; 37:821–826. [PubMed: 12628172]

Mellen NM, Mishra D. Functional anatomical evidence for respiratory rhythmogenic function of endogenous bursters in rat medulla. J Neurosci. 2010; 30:8383–8392. [PubMed: 20573885]

Mellen NM, Thoby-Brisson M. Respiratory circuits: development, function and models. Current opinion in neurobiology. 2012; 22:676–685. [PubMed: 22281058]

Montandon G, Horner R. CrossTalk proposal: The preBötzinger complex is essential for the respiratory depression following systemic administration of opioid analgesics. The Journal of physiology. 2014; 592:1159–1162. [PubMed: 24634011]

Montandon G, Qin W, Liu H, Ren J, Greer JJ, Horner RL. PreBotzinger complex neurokinin-1 receptor-expressing neurons mediate opioid-induced respiratory depression. The Journal of neuroscience : the official journal of the Society for Neuroscience. 2011; 31:1292–1301. [PubMed: 21273414]

Onimaru H, Homma I. A novel functional neuron group for respiratory rhythm generation in the ventral medulla. The Journal of neuroscience : the official journal of the Society for Neuroscience. 2003; 23:1478–1486. [PubMed: 12598636]

Pepper J, Braude S, Lacey E, Sherman P. Vocalizations of the naked mole-rat. The biology of the naked mole-rat. 1991:243–274.

Pierani A, Moran-Rivard L, Sunshine MJ, Littman DR, Goulding M, Jessell TM. Control of interneuron fate in the developing spinal cord by the progenitor homeodomain protein Dbx1. Neuron. 2001; 29:367–384. [PubMed: 11239429]

Portfors CV. Types and functions of ultrasonic vocalizations in laboratory rats and mice. Journal of the American Association for Laboratory Animal Science. 2007; 46:28–34. [PubMed: 17203913]

Ramírez-Jarquín JO, Lara-Hernández S, Lopez-Guerrero JJ, Aguileta MA, Rivera-Angulo AJ, Sampieri A, Vaca L, Ordaz B, Pena-Ortega F. Somatostatin modulates generation of inspiratory rhythms and determines asphyxia survival. Peptides. 2012; 34:360–372. [PubMed: 22386651]

Riede T. Stereotypic Laryngeal and Respiratory Motor Patterns Generate Different Call Types in Rat Ultrasound Vocalization. Journal of Experimental Zoology Part A: Ecological Genetics and Physiology. 2013

Rossi J, Balthasar N, Olson D, Scott M, Berglund E, Lee CE, Choi MJ, Lauzon D, Lowell BB, Elmquist JK. Melanocortin-4 receptors expressed by cholinergic neurons regulate energy balance and glucose homeostasis. Cell Metab. 2011; 13:195–204. [PubMed: 21284986]

Ruangkittisakul A, Schwarzacher SW, Secchia L, Ma Y, Bobocea N, Poon BY, Funk GD, Ballanyi K. Generation of eupnea and sighs by a spatiochemically organized inspiratory network. J Neurosci. 2008; 28:2447–2458. [PubMed: 18322090]

Rubsamen R. Ontogenesis of the echolocation system in the rufous horseshoe bat, Rhinolophus rouxi (audition and vocalization in early postnatal development). Journal of Comparative Physiology A. 1987; 161:899–913.

Schneider CA, Rasband WS, Eliceiri KW. NIH Image to ImageJ: 25 years of image analysis. Nat Methods. 2012; 9:671–675. [PubMed: 22930834]

Smith JC, Ellenberger HH, Ballanyi K, Richter DW, Feldman JL. Pre-Botzinger complex: a brainstem region that may generate respiratory rhythm in mammals. Science. 1991; 254:726–729. [PubMed: 1683005]

Smotherman MS. Sensory feedback control of mammalian vocalizations. Behavioural brain research. 2007; 182:315–326. [PubMed: 17449116]

Stornetta RL, Rosin DL, Wang H, Sevigny CP, Weston MC, Guyenet PG. A group of glutamatergic interneurons expressing high levels of both neurokinin-1 receptors and somatostatin identifies the region of the pre-Botzinger complex. The Journal of Comparative Neurology. 2003; 455:499–512. [PubMed: 12508323]

Taber-Pierce E, Lichentenstein E, Feldman SC. The somatostatin systems of the guinea-pig brainstem. Neuroscience. 1985; 15:215–235. [PubMed: 2861583]

Tachibana M, Rothman JM, Guth PS. Somatostatin along the auditory pathway. Hear Res. 1979; 1:365–368. [PubMed: 44284]

Tan W, Janczewski WA, Yang P, Shao XM, Callaway EM, Feldman JL. Silencing preBotzinger Complex somatostatin-expressing neurons induces persistent apnea in awake rat. Nat Neurosci. 2008; 11:538–540. [PubMed: 18391943]

Tanaka DH, Oiwa R, Sasaki E, Nakajima K. Changes in cortical interneuron migration contribute to the evolution of the neocortex. Proceedings of the National Academy of Sciences of the United States of America. 2011; 108:8015–8020. [PubMed: 21518872]

Taniguchi H, He M, Wu P, Kim S, Paik R, Sugino K, Kvitsiani D, Fu Y, Lu J, Lin Y, Miyoshi G, Shima Y, Fishell G, Nelson SB, Huang ZJ. A resource of Cre driver lines for genetic targeting of GABAergic neurons in cerebral cortex. Neuron. 2011; 71:995–1013. [PubMed: 21943598]

Telgkamp P, Cao YQ, Basbaum AI, Ramirez JM. Long-term deprivation of substance P in PPT-A mutant mice alters the anoxic response of the isolated respiratory network. J Neurophysiol. 2002; 88:206–213. [PubMed: 12091546]

Thoby-Brisson M, Trinh JB, Champagnat J, Fortin G. Emergence of the pre-Botzinger respiratory rhythm generator in the mouse embryo. J Neurosci. 2005; 25:4307–4318. [PubMed: 15858057]

Tong Q, Ye C, McCrimmon RJ, Dhillon H, Choi B, Kramer MD, Yu J, Yang Z, Christiansen LM, Lee CE, Choi CS, Zigman JM, Shulman GI, Sherwin RS, Elmquist JK, Lowell BB. Synaptic Glutamate Release by Ventromedial Hypothalamic Neurons Is Part of the Neurocircuitry that Prevents Hypoglycemia. Cell Metab. 2007; 5:383–393. [PubMed: 17488640]

Tupal S, Huang WH, Picardo MC, Ling GY, Del Negro C, Zoghbi HY, Gray PA. Atoh1-dependent rhombic lip neurons are required for temporal delay between independent respiratory oscillators in embryonic mice. Elife. 2014 in press.

Van Daele DJ, Cassell MD. Multiple forebrain systems converge on motor neurons innervating the thyroarytenoid muscle. Neuroscience. 2009; 162:501–524. [PubMed: 19426785]

Van Daele DJ, Fazan VP, Agassandian K, Cassell MD. Amygdala connections with jaw, tongue and laryngo-pharyngeal premotor neurons. Neuroscience. 2011; 177:93–113. [PubMed: 21211549]

Wallen-Mackenzie A, Gezelius H, Thoby-Brisson M, Nygard A, Enjin A, Fujiyama F, Fortin G, Kullander K. Vesicular glutamate transporter 2 is required for central respiratory rhythm generation but not for locomotor central pattern generation. J Neurosci. 2006; 26:12294–12307. [PubMed: 17122055]

Wallen-Mackenzie A, Wootz H, Englund H. Genetic inactivation of the vesicular glutamate transporter 2 (VGLUT2) in the mouse: what have we learnt about functional glutamatergic neurotransmission? Upsala journal of medical sciences. 2010; 115:11–20. [PubMed: 20187846]

Wang X, Hayes JA, Picardo MC, Del Negro CA. Automated cell-specific laser detection and ablation of neural circuits in neonatal brain tissue. The Journal of physiology. 2013; 591:2393–2401. [PubMed: 23440965]

Wenninger JM, Pan LG, Klum L, Leekley T, Bastastic J, Hodges MR, Feroah T, Davis S, Forster HV. Small reduction of neurokinin-1 receptor-expressing neurons in the pre-Botzinger complex area induces abnormal breathing periods in awake goats. J Appl Physiol. 2004a; 97:1620–1628. [PubMed: 15247160]

Wenninger JM, Pan LG, Klum L, Leekley T, Bastastic J, Hodges MR, Feroah TR, Davis S, Forster HV. Large lesions in the pre-Botzinger complex area eliminate eupneic respiratory rhythm in awake goats. J Appl Physiol. 2004b; 97:1629–1636. [PubMed: 15247161]

Wild J, Goller F, Suthers R. Inspiratory muscle activity during bird song. Journal of neurobiology. 1998; 36:441. [PubMed: 9733078]

Wonders CP, Anderson SA. The origin and specification of cortical interneurons. Nature reviews. Neuroscience. 2006; 7:687–696.

Yosida S, Kobayasi KI, Ikebuchi M, Ozaki R, Okanoya K. Antiphonal Vocalization of a Subterranean Rodent, the Naked Mole Rat (Heterocephalus glaber). Ethology. 2007; 113:703–710.

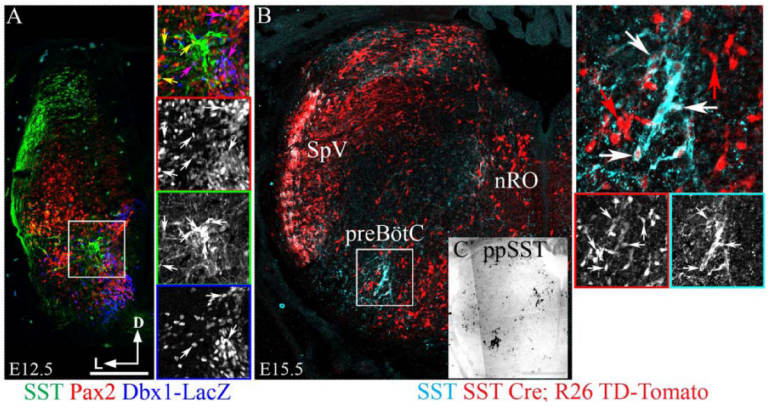

Figure 1.

Development of preBötC SST expression. (A) Confocal mosaic image showing expression of SST (green), Pax2 (red) and LacZ (blue) in an E12.5 *Dbx1*-LacZ mouse medulla. Inset expanded to right. Arrow color indicates extent of co-expression. Note absence of SST and LacZ co-expression. (B) Confocal mosaic image showing co-localization of SST with TD-Tomato within the preBötC of an E15.5 SST-Cre;R26TD-Tomato transgenic mouse. Inset expanded to right. (C) Mosaic image showing *in situ* hybridization of preproSST mRNA in adjacent section from B. Scale bar, 200 μm (A and B), 400 μm (C).

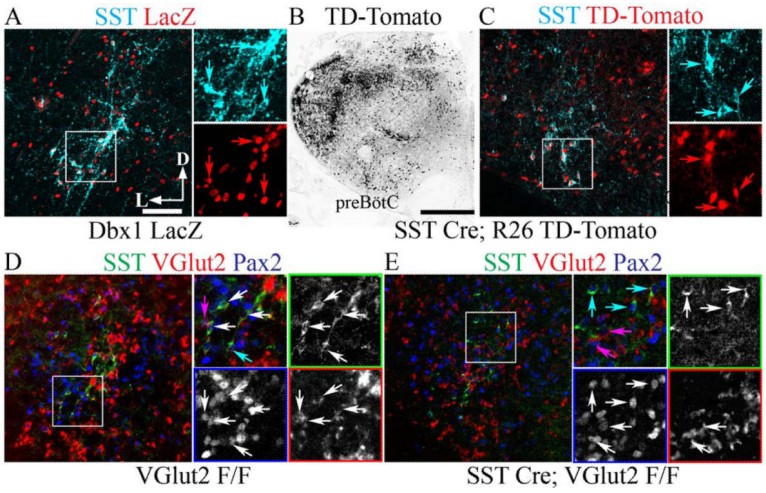

Figure 2.

SST-Cre eliminates VGlut2 mRNA from preBötzinger Complex SST neurons. Confocal immunofluorescent images showing co-expression of high levels of cell body SST peptide within the P0 mouse preBötC. (A) SST peptide (cyan) co-expression with LacZ (red) in *Dbx1*$^{LacZ/+}$ mouse. Inset expanded to right showing single-color images. Arrows indicate co-expression. (B) Broad TD-Tomato expression (black) in SST-Cre;R26TD-Tomato mouse. (C) SST peptide (cyan) co-expression with TD-Tomato (red) in SST-Cre;R26TD-Tomato preBötC. Inset expanded to right showing single-color images. Arrows indicate co-expression. (D) Co-expression of SST (green) with VGlut2 mRNA (inverted and pseudocolored red) and Pax2 (blue) in VGlut2$^{F/F}$ mouse. Inset expanded to right showing single-color images (colored squares). White arrows indicate triple co-expression. Magenta arrow indicates VGlut2 and Pax2 co-expression. (E) Loss of co-expression of SST with VGlut2 mRNA (red) and Pax2 (blue) in SST-Cre;VGlut2$^{F/F}$ mouse. Inset expanded to right showing single-color images (colored squares). Magenta arrows indicate VGlut2 and Pax2 co-expression. Cyan arrows indicate SST and Pax2 co-expression. Note the absence of co-localization of SST with VGlut2 indicating efficient genetic ablation. Scale bars, 100 μm (A), 500 μm (B).

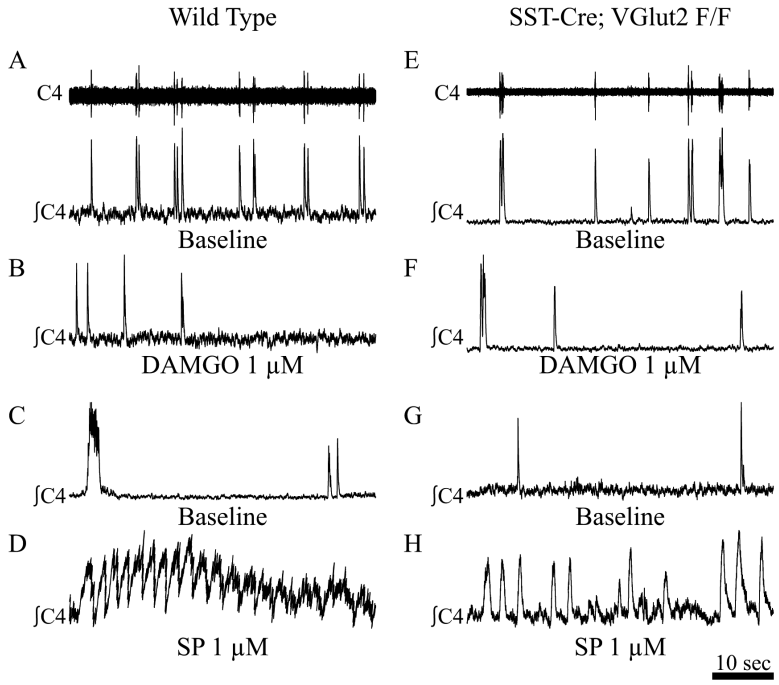

Figure 3.

Silencing preBötC SST neurons does not affect breathing *in vitro*. C4 root recordings (A and E, upper, raw; lower, integrated) of endogenous inspiratory output from P0 control (A–D) and SST-Cre;VGlut2$^{F/F}$ (E–H) medulla–spinal cord preparations under baseline conditions (A, C, E, G) or in the presence of bath-applied DAMGO (1 μM; B and F) or SP (1 μM; D and H). Scale bar, 10 s.

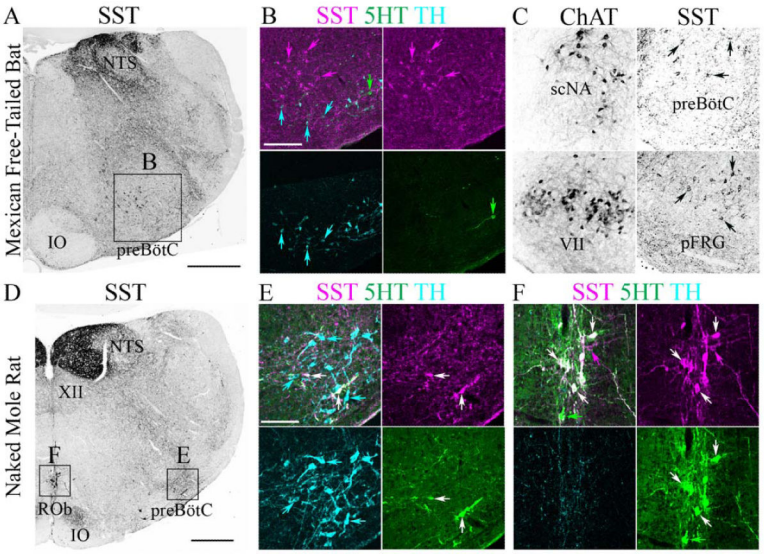

Figure 4.

PreBötC SST expression is species-dependent. Inverted confocal mosaic images of SST peptide expression at the level of the preBötC in (A) adult Mexican fruit bat and (D) naked mole-rat. (B) Three-color confocal mosaics (upper left) and single-color images showing SST (magenta), 5HT (green) and TH (cyan) expression within the bat preBötC (expanded from A). Bats show many SST-positive neurons specifically within the preBötC. (C) Inverted confocal mosaic images of ChAT (left) and SST peptide expression (right) showing extension of SST population from caudal pole of preBötC (upper) to the pFRG region (lower) in bat. (E and F) Three-color confocal mosaics (upper left) and single color images showing SST (magenta), 5HT (green) and TH (cyan) expression within the naked mole-rat preBötC (E, expanded from D) and raphe obscurus (F, expanded from D). Naked mole-rats show co-expression of SST in 5HT neurons, but not within preBötC. Arrows indicate SST-positive cell bodies. Scale bars, 500 μm (A and D), 100 μm (in B for B and C, and in E for E and F).

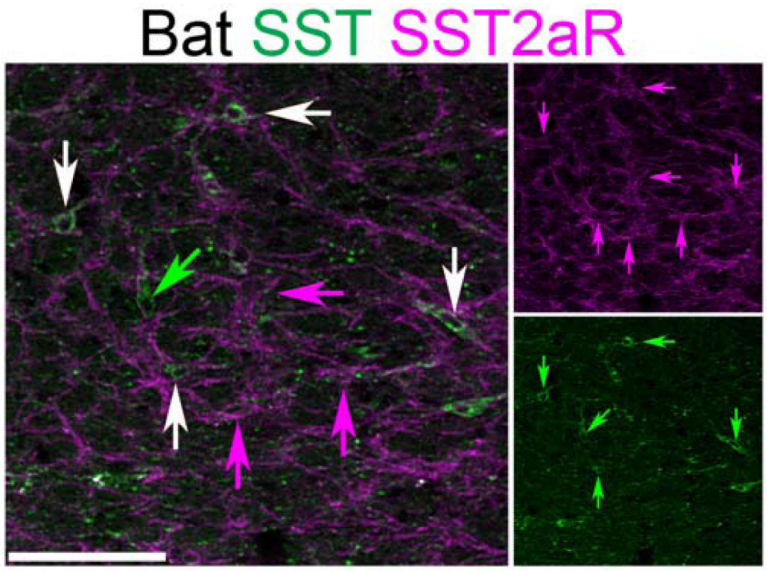

Figure 5.

Bat ventrolateral medulla SST neurons co-express SST2aR. Two-color confocal projection images showing partial co-expression of SST (green) and SST2aR (magenta) within the approximate region of the bat preBötC. Single-color images are shown to right. White arrows indicate SST and SST2aR co-expression. Green arrow indicates SST neuron lacking SST2aR expression. Magenta arrows indicate SST2aR neurons lacking SST expression. Scale bar, 100 μm.

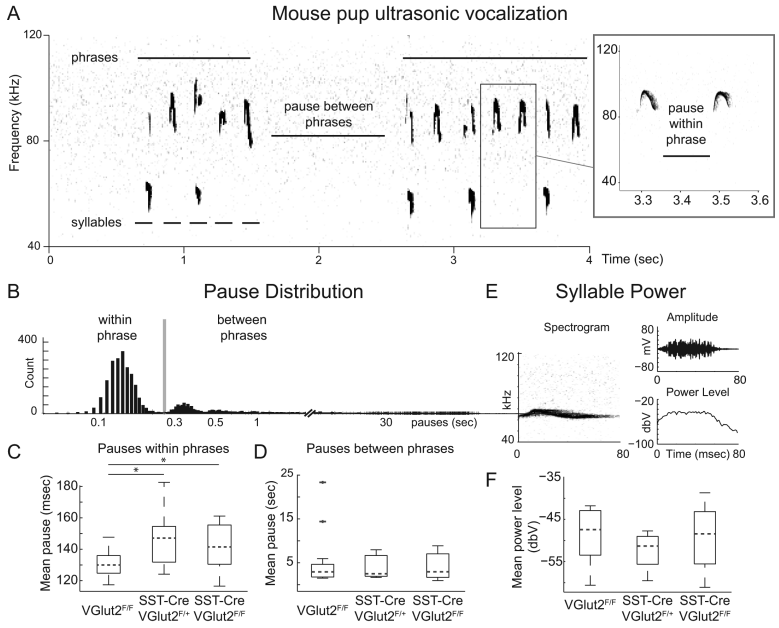

Figure 6.

Loss of glutamate release from SST neurons increases inspiratory pause time between syllables. (A) Example of 4s of ultrasonic spectrogram (kHz) from a P8 VGlut2$^{F/F}$ control mouse showing two bouts (phrases) of calling separated by a between-phrase pause. Each phrase consists of multiple syllables, indicated by lower bars. Inset right, expanded from box, shows two syllables and a single within-phrase pause. (B) Distribution of pause length (in s; log spacing) between syllables for all genotypes combined (4037 total syllables) showing cutoff (grey bar, 0.24 s) for within- or between-phase pauses. (C) Boxplot showing average of within-phrase pause times for each genotype (VGlut2$^{F/F}$, SST-Cre;VGlut2$^{F/+}$ and SST-Cre;VGlut2$^{F/F}$). Within-phrase pause times for both SST-Cre;VGlut2$^{F/+}$ (*P = 0.01, Bonferroni-corrected) and SST-Cre;VGlut2$^{F/F}$ (*P = 0.02, Bonferroni-corrected) were statistically significantly longer than control (VGlut2$^{F/F}$). (D) Boxplot of average between-phrase pauses showing no significant differences between groups. (E) Example of 80-ms ultrasonic spectrogram (left) and corresponding changes in microphone amplitude (upper right; mV) and power level (lower right; dbV). (F) Boxplot showing no significant differences between genotypes time-averaged syllable power, related to average syllable loudness.